

## Reactivity of Chloro(phthalocyaninato)iron(III) in Pyridine–Water

Fabrizio Monacelli

Dipartimento di Chimica, Università di Roma 'La Sapienza', p. le A. Moro 6, 00185 Roma, Italy

The reaction of  $[\text{Fe}(\text{pc})\text{Cl}]$  (pc = phthalocyaninate) in water-containing pyridine (py) has been followed by spectrophotometric and conductometric techniques. It is a two-step process: the first step is first-order on  $[\text{H}_2\text{O}]$  and is accompanied by an increase in conductance, the second is kinetically independent of water and does not involve ionic species. The complex  $[\text{Fe}(\text{pc})(\text{py})_2]$  is formed during both steps and about 70–80% of the initial iron(III) is finally recovered in this form. The infinite-time conductance is quantitatively explained in terms of 100% formation of  $\text{py}\cdot\text{HCl}$ . Addition of  $\text{PPh}_3$  has a remarkable effect: when added to py *before*  $[\text{Fe}(\text{pc})\text{Cl}]$  the second step tends to vanish as the concentration of  $\text{PPh}_3$  increases and, for  $[\text{PPh}_3] \geq 4 \times 10^{-3} \text{ mol dm}^{-3}$  the overall reaction appears as a one-step process; if the phosphine is added *after* the first step and *before* the second, two consecutive reactions take place, the first kinetically phosphine-dependent, the second independent of  $\text{PPh}_3$ . Virtually quantitative oxidation to  $\text{OPPh}_3$  occurs when the complex is allowed to react with a slight excess of  $\text{PPh}_3$ . The observations are explained in terms of a rapid  $\text{Cl}^-$  release from  $[\text{Fe}(\text{pc})\text{Cl}(\text{py})]$  to give  $[\text{Fe}(\text{pc})(\text{py})_2]^+$ ,  $\text{Cl}^-$  which, in turn, undergoes substitution of an axial py by water. A hydroxo species forms which readily dimerises and the dimer disproportionates to give  $[\text{Fe}(\text{pc})(\text{py})_2]$  and the iron(IV) species  $[\text{Fe}(\text{pc})\text{O}(\text{py})]$ . Considerations based on the instability of analogous oxoporphyrinatoiron(IV) species and on the nearly 75% overall yield of  $[\text{Fe}(\text{pc})(\text{py})_2]$  lead to the suggestion that the iron(IV) compound is in the form of a  $\mu$ -peroxo or di- $\mu$ -oxo dimer.

In 1938 Barrett *et al.*<sup>1</sup> reported the preparation of a Cl-containing compound obtained by air-refluxing a suspension of phthalocyaninatoiron(II)  $[\text{Fe}(\text{pc})]$  in concentrated aqueous HCl. This compound was considered to be a phthalocyaninatoiron(III) derivative containing a  $\text{Cl}^-$  anion. For a long time the very nature of this material has been debated. Pieces of evidence were collected in favour of the formula  $[\text{Fe}(\text{pc})\text{Cl}]$ <sup>2–6</sup> but some authors favoured a hydrochloride salt of phthalocyaninatoiron(II)  $[\text{Fe}(\text{pc})]\cdot\text{HCl}$ ,<sup>7,8</sup> obviously indistinguishable from the former on the basis of analytical data only.

More recently, the preparation and characterisation of a bis(hydroxo)- and of a series of bis(alkoxo)-phthalocyaninatoiron(III) salts have been reported.<sup>9</sup> Their reaction with hydrogen chloride was found to yield a monochloro derivative identical to the Barrett compound. This same product was also obtained by treating the well characterised  $\mu$ -oxo-bis[phthalocyaninatoiron(III)] with HCl in  $\text{CH}_2\text{Cl}_2$ . Analogous behaviour was observed when using any other hydrogen halide. Finally, the Mössbauer spectrum of the compound  $[\{\text{Fe}(\text{pc})\text{Cl}\}_2\text{I}_2]$ , whose X-ray structure demonstrates the presence of  $\text{I}_2$ -bridged  $\text{Fe}^{\text{III}}(\text{pc})\text{Cl}$  pyramids, was found to be nearly identical to that of  $[\text{Fe}(\text{pc})\text{Cl}]$ .<sup>10</sup> These results are hardly in agreement with the hydrochloride formulation while they are consistent with the  $[\text{Fe}(\text{pc})\text{Cl}]$  alternative. In conclusion, despite previous different claims, there is now little doubt that the material prepared by the Barrett method,<sup>1</sup> as well as *via* alternative routes,<sup>9</sup> is a true five-co-ordinate chloro(phthalocyaninato)iron(III),  $s = \frac{3}{2}/s = \frac{5}{2}$  spin admixed<sup>11</sup> complex.

Most work on chloro(phthalocyaninato)iron(III) has been limited to the analysis of spectral and magnetic properties, with no specific attention to its reactivity. Thus, it was considered of particular interest to investigate this aspect starting with the reaction occurring when the complex is dissolved in pyridine. A parallel investigation concerned the reactivity of  $\mu$ -oxo-bis[phthalocyaninatoiron(III)] in the same medium.<sup>12</sup> Although this system is more complex than the one here described, it shows common aspects that made useful a parallel study of both compounds.

### Experimental

**Materials.**—Chloro(phthalocyaninato)iron(III) was prepared according to the method described by Barrett.<sup>1</sup> The elemental analyses were as expected and the IR spectrum identical to that reported in the literature.<sup>4</sup> This preparation was repeated several times with no differences in the properties of the material collected and/or its reactivity.

Pyridine was usually an RPE-ACS C. Erba reagent and was distilled at least three times on BaO, under a UPP nitrogen stream. The purified pyridine was kept under dry nitrogen and much care was used in avoiding any direct contact with the atmosphere. As a rule, the stock pyridine was renewed monthly.

**Instruments.**—Spectrophotometric measurements were carried out on a Perkin-Elmer 555 spectrophotometer and on a Beckman DU 8 instrument. The first was preferred when a wavelength range had to be explored while the second was essentially used for kinetic measurements at a single wavelength. A Hewlett-Packard diode-array 8452 A spectrophotometer was used for simultaneous readings over the range 400–750 nm.

Conductivity experiments were carried out with a AMEL 133 conductivity meter connected to a recorder. Coupled conductivity and spectrophotometric measurements were performed with an especially designed spectrophotometric cell provided with a couple of platinum electrodes. The cell was calibrated by conventional procedures and the corresponding constant was found to be  $0.258 \text{ cm}^{-1}$ . This same cell was used for conductometric experiments with no parallel measure of the optical density. In this case, control of temperature was achieved by immersing the cell in a thermostatted paraffin oil-bath.

**Mixing device and kinetic procedure.** Chloro(phthalocyaninato)iron(III) is a deep green powder which had to be dissolved, and the solution filtered, prior to each experiment. Due to the lability of the complex and its sensitivity to water (see below), dissolution and filtration had to be accomplished in a few seconds and with the minimum contact with air moisture.

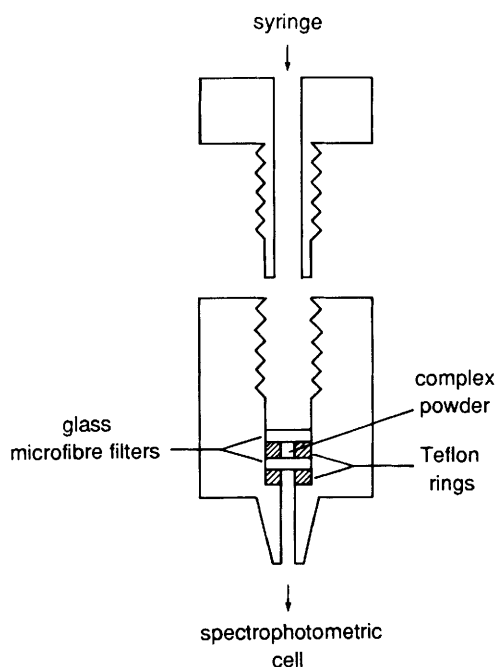


Fig. 1 Filtering device for quick preparation of the reaction solutions

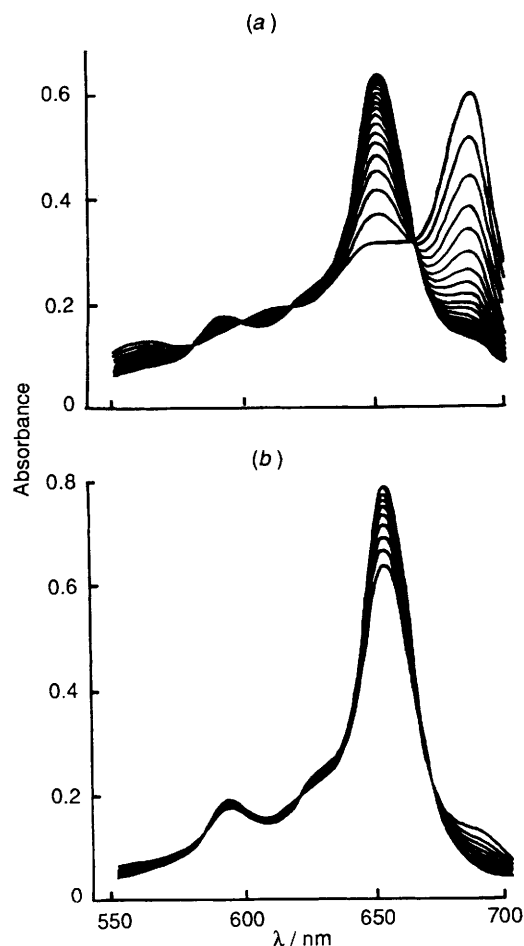


Fig. 2 Spectral evolution of a pyridine solution of  $[\text{Fe}(\text{pc})\text{Cl}]$  (without addition of water) in the range 550–700 nm at 35 °C. (a) First step, (b) second step. Time intervals between two consecutive spectra: 2 min (a) and 10 min (b)

Both goals were attained by using the simple device shown in Fig. 1. The all-Teflon cartridge, fittable to a commercial glass syringe, was filled with a small amount of the solid compound. A

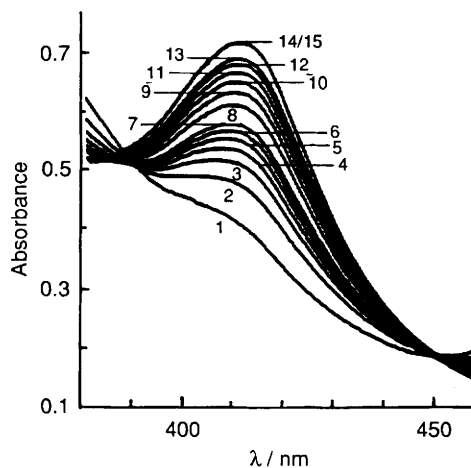


Fig. 3 Spectral evolution of a pyridine solution of  $[\text{Fe}(\text{pc})\text{Cl}]$  (without addition of water) in the range 380–460 nm at 35 °C. Time intervals between two consecutive spectra: 5 (spectra 1–7, first step) and 15 min (spectra 7–13, second step). Spectra 14 and 15 are superimposed and were recorded after 10 and 12 h, respectively

5 cm<sup>3</sup> syringe, the tip of which had previously been occluded with a little silicon grease, was filled with the necessary amount of pyridine containing a known concentration of water. External circulation of thermostatted water ensured temperature control. The syringe was then connected to the Teflon cartridge and, after thermal equilibration, gentle pressure on the piston made the pyridine to flow through and dissolve the iron complex on contact. The undissolved material was retained by a glass microfibre filter (Whatman) and the clear solution could readily be collected in the spectrophotometric cell. No more than 5 s from mixing were required before starting with the absorbance readings. This dead time and the consequent temperature perturbation, while unimportant in all the runs reported here, precluded the possibility of exploring faster rates, thus setting an upper limit to the concentration of water (see below).

The cell path length was from 0.1 to 1.0 cm and, accordingly, the concentration of the iron complex varied from  $ca. 2 \times 10^{-4}$  to  $ca. 5 \times 10^{-6}$  mol dm<sup>-3</sup>.

Unless otherwise stated, all measurements were carried out at  $35.0 \pm 0.1$  °C. The experiments were designed so as to record periodically either the spectrum within a given range of wavelengths (usually 550–700 nm) or the absorbance at a fixed wavelength (688 or 653 nm).

## Results

**Spectral Changes.**—The spectral evolution of an  $[\text{Fe}(\text{pc})\text{Cl}]$  solution in carefully purified pyridine *without addition of water* (see below) is shown in Figs. 2 and 3. The first spectrum recorded soon after mixing is characterised by a strong band at 688 nm which eventually decreases in intensity while the 653 and 414 nm bands start growing up.

With the exclusion of the first spectrum (which may reasonably suffer a small temperature perturbation, see Experimental section) the isothermal sequence of spectra recorded within the first few minutes [Fig. 2(a)] shows sharp isobestics at 581, 598, 619 and 667 nm. This indicates that a well defined process is taking place with a coloured species changing to another coloured species (or a constant composition mixture) without appreciable accumulation of intermediates. Owing to the velocity of the changes observed as compared with the scanning rate and the dead time, the shoulder at 655 nm in the first spectrum is due, at least in part, to the formation of the species absorbing at 653 nm.

When the absorbance at 688 nm is close to its minimum the absorbance at 653 nm is still increasing considerably [see Fig.

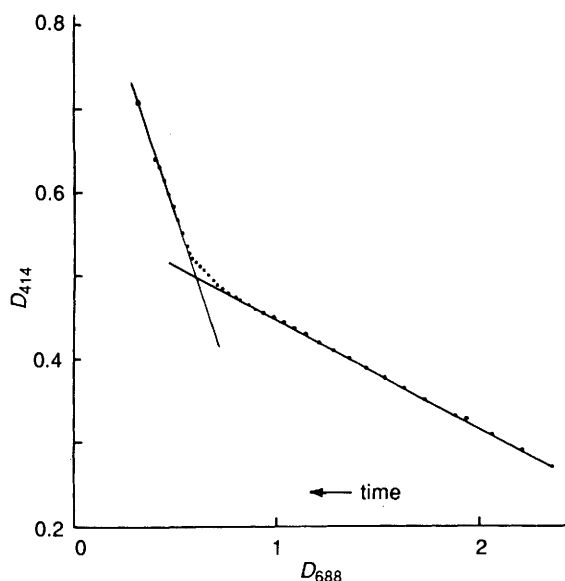


Fig. 4 Optical absorbance at 414 nm *vs.* the absorbance at 688 nm (taken simultaneously) for a pyridine solution of  $[\text{Fe}(\text{pc})\text{Cl}]$  at 25 °C

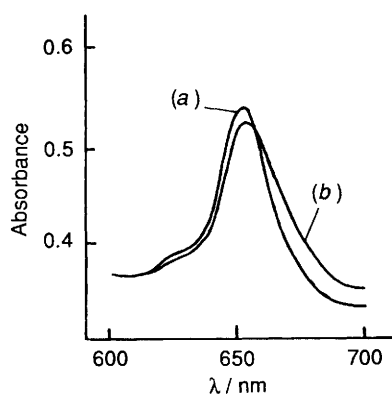


Fig. 5 Spectra at the end of the first step:  $[\text{H}_2\text{O}] = 0.55$  (a) and  $8.3 \text{ mol dm}^{-3}$  (b). The spectra are normalised to the same final  $[\text{Fe}(\text{pc})(\text{py})_2]$  concentration

2(b)]. This suggests that, while the disappearance of the band at 688 nm is a one-step process, the growth of the absorption at 653 nm occurs in two consecutive steps. This is also confirmed by the growth of the maximum at 414 nm which clearly occurs in two successive steps on a different time-scale (Fig. 3). This situation is more clearly shown by the two-arm shape of the plot of Fig. 4 where the absorbance at 414 nm is plotted *versus* the simultaneous absorbance at 688 nm. Hence, Fig. 2(a) and spectra 1–7 of Fig. 3 refer essentially to the first step, whilst the spectral changes shown in Fig. 2(b) and those at later times in Fig. 3 are due mainly to the second.

Addition of small amounts of water to the reaction mixture does not alter the picture except that it makes the first step faster. Indeed, upon addition of more than  $20 \mu\text{l cm}^{-3}$  of water ( $[\text{H}_2\text{O}] > 1 \text{ mol dm}^{-3}$ ) the first step is virtually complete within the time of mixing and thus the changes observed after mixing refer to the second step.

On increasing the water concentration the shape of the band at 653 nm at the end of the first step becomes increasingly

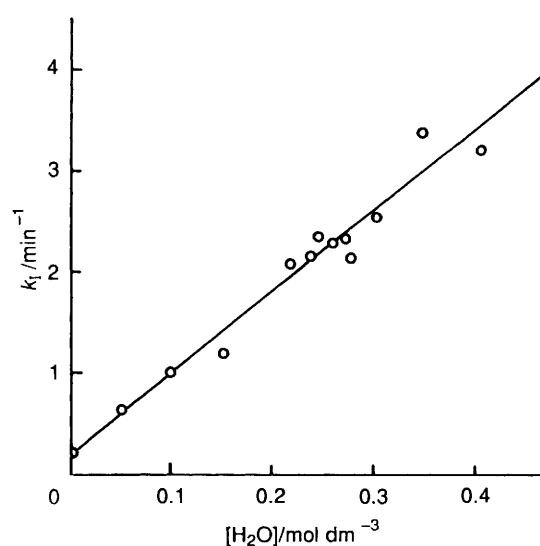


Fig. 6 Pseudo-first-order rate constant  $k_1$  as a function of water concentration. The point at zero water concentration is the average of ten independent values

asymmetric with a slight red-shift of the maximum (Fig. 5). In all cases the spectrum at the end of the second step was identical to that of a solution of  $[\text{Fe}(\text{pc})(\text{py})_2]$  ( $\text{py} = \text{pyridine}$ ). Especially designed experiments\* demonstrate that only about  $82 \pm 2\%$  of the starting iron is recovered as  $[\text{Fe}(\text{pc})(\text{py})_2]$ . This amount is practically insensitive to water ( $79 \pm 2\%$  up to  $[\text{H}_2\text{O}] = 5.5 \text{ mol dm}^{-3}$ ).

The addition of triphenylphosphine to the solutions containing  $[\text{Fe}(\text{pc})\text{Cl}]$  has remarkable effects: above *ca.*  $5 \times 10^{-4} \text{ mol dm}^{-3}$  of  $\text{PPh}_3$  the yield of  $[\text{Fe}(\text{pc})(\text{py})_2]$  reaches its stoichiometric 100% limit while the process tends progressively to resemble a one-step, first-order reaction (see below).

**Kinetics.—The first step.** The two consecutive steps are overlapped to an extent which depends on their relative rates. Since the first step is considerably faster than the second, and becomes increasingly so with the water content of the solution, it could be readily resolved by extrapolating, on an absorbance *vs.* time plot, the linear 'tail' due to the second step, according to a well known graphical method.<sup>14</sup> In all cases good first-order plots were obtained over two or more half-lives.

Fairly good linear plots were also obtained with the Guggenheim method<sup>15</sup> and, although the time interval chosen,  $\Delta t$ , was much smaller than the half-life,<sup>15</sup> both methods, when applied together, gave consistent results. In some cases, because of accidental lack of data for the final part of the reaction, the Guggenheim method was the only procedure available for computing the rate constant,  $k_1$ , of the first step. The results obtained are shown in Fig. 6. It is clear that  $k_1$  is a linear function of water concentration. Least-squares analysis of the data yields  $k_1 = 0.20 + 7.9[\text{H}_2\text{O}] \text{ min}^{-1}$ .

**The second step.** The optical data referring to the final stage of the reaction do not conform to a simple first-order law, for the plots of  $-\ln(D_f - D_t)$  *vs.* time at 653 nm ( $D_f$  and  $D_t$  are the absorbances at equilibrium and at time  $t$ , respectively) show a marked upwards curvature. In spite of the relatively narrow range of absorbance covered [see Fig. 2(b)] and the correspondingly low accuracy of the differences  $D_f - D_t$ , this behaviour must be regarded as an intrinsic feature of the kinetics under study. Nor can it be due to interference from the first step because this would result in a downward curvature and addition of water in amounts large enough to complete the first step within the time of mixing does not modify this situation.

Despite the relatively complex kinetic behaviour, the presence of several isobestics [Fig. 2(b)] indicates, also for this second step, a simple stoichiometry.

\* The absorption coefficient of  $[\text{Fe}(\text{pc})(\text{py})_2]$  at 653 nm was measured accurately at 35 °C and found to be  $\epsilon_{653} = (1.20 \pm 0.05) \times 10^5 \text{ dm}^3 \text{ mol}^{-1} \text{ cm}^{-1}$ . This value, which compares satisfactorily with that reported in the literature<sup>13</sup> ( $\epsilon_{653} = 1.3 \times 10^5 \text{ dm}^3 \text{ mol}^{-1} \text{ cm}^{-1}$ ) was used to calculate the final concentration of  $[\text{Fe}(\text{pc})(\text{py})_2]$  of solutions obtained by dissolving accurately weighed samples of  $[\text{Fe}(\text{pc})\text{Cl}]$ .

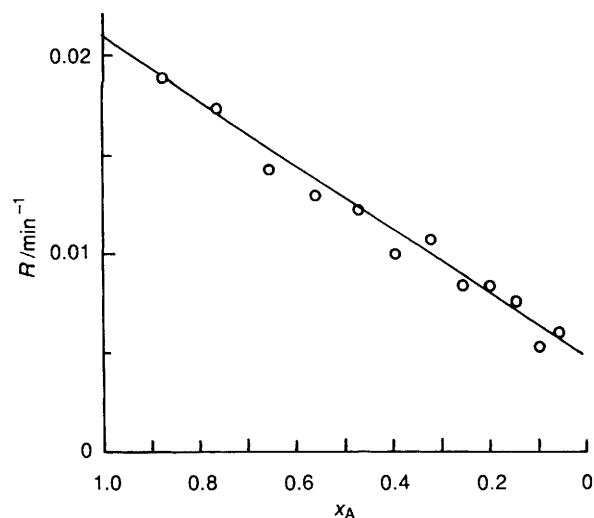


Fig. 7 Second step. Normalised instantaneous rate  $R$  as a function of the mole fraction of the reacting species

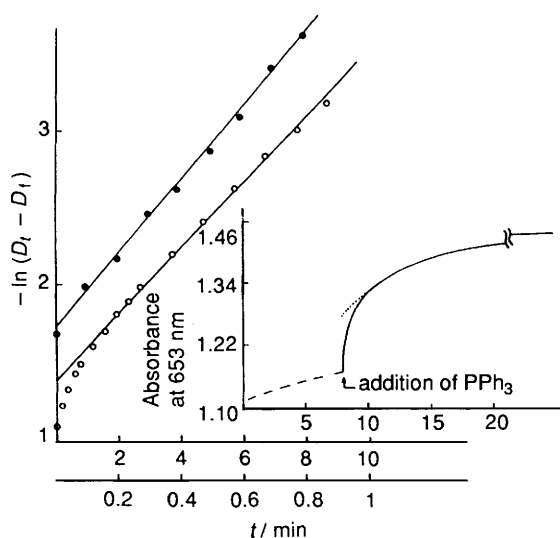


Fig. 8 First-order plots for the reactions taking place upon addition of  $\text{PPh}_3$  at the end of the first step. The inset shows the increase in absorbance at 653 nm due to the final part of the first step and the beginning of the second (dashed line), and the sudden increase after addition of  $\text{PPh}_3$  (solid line). Also shown is the corresponding first-order plot (empty circles, upper time-scale). The initial deviation is assumed to be due to a preceding faster process, the rate constant of which may be calculated as the slope of the upper straight line (filled circles, lower time-scale) according to the procedure described in ref. 14.  $[\text{H}_2\text{O}] = 0.27$ ;  $[\text{PPh}_3] = 1.9 \times 10^{-5} \text{ mol dm}^{-3}$ ;  $35^\circ\text{C}$

Fig. 7 shows, for a representative run, a plot of the normalised instantaneous\* rate  $R = -(dD_t/dt)/(D_i - D_f)$  vs.  $x_A$ , where  $x_A = (D_i - D_t)/(D_i - D_f)$  and  $D_i$  is the initial absorbance. If the observed process were a simple first-order reaction of the type  $\text{A} \rightarrow \text{B}$ ,  $x_A$  would be identified with the mole fraction of A at any time and  $R$  with the instantaneous rate of the reaction  $dx_A/dt$ , the quantities being related by the linear equation (1).

$$R = -dx_A/dt = k_{II}x_A \quad (1)$$

Fig. 7 shows that  $R$  is indeed a linear function of  $x_A$  but the intercept at  $x_A = 0$  is definitely non-zero. Thus, the kinetic

equation describing the second step seems to be (2) where a zero-

$$-dx_A/dt = k_{II}x_A + b \quad (2)$$

order term, corresponding to the intercept  $b$ , is introduced. Since the evaluation of  $x_A$  requires a relatively accurate value for  $D_i$ , only those runs where the first step was virtually instantaneous (*i.e.* for  $[\text{H}_2\text{O}] > 0.5 \text{ mol dm}^{-3}$ ) could be analysed according to equation (2). For the runs at lower  $[\text{H}_2\text{O}]$  the following procedure was adopted. Equation (2) may be integrated and, after straightforward manipulations, put in the logarithmic form (3) where  $D_f' = D_f + b(D_f - D_i)/k_{II}$ . Of course,  $D_f'$  is unknown but can be found by a trial-and-error procedure until a satisfactory linearisation of the plot of equation (3) is obtained, the slope of which is again  $k_{II}$ . When

$$-\ln(D_i - D_f') = k_{II}t + \text{constant} \quad (3)$$

applied together, both procedures gave consistent results (within  $\pm 10\%$  or better). The values of both  $k_{II}$  and  $b$  are poorly reproducible [ $k_{II} = 0.027 \pm 0.019 \text{ min}^{-1}$ ,  $b = (4.4 \pm 1.7) \times 10^{-3} \text{ min}^{-1}$ ] and do not seem to show any definite trend either with water concentration or with the initial concentration of  $[\text{Fe}(\text{pc})\text{Cl}]$ .

*Effect of added triphenylphosphine.* Experiments were carried out in which  $[\text{Fe}(\text{pc})\text{Cl}]$  was allowed to react with water-pyridine in the presence of variable amounts of  $\text{PPh}_3$  (type A experiments) or the phosphine was added after the first step had reached completion (type B experiments). In both cases the presence of the phosphine had a remarkable effect.

*Type A experiments.* Increasing amounts of  $\text{PPh}_3$ , from *ca.*  $5 \times 10^{-4}$  to  $4 \times 10^{-3} \text{ mol dm}^{-3}$ , were dissolved in pure pyridine (no water added) and the solution used in kinetic experiments. The most striking effect was a progressive disappearance of the second step and, for  $[\text{PPh}_3] \geq 4 \times 10^{-3} \text{ mol dm}^{-3}$ , the reaction appeared to develop in only one step. This process was first order in  $[\text{Fe}(\text{pc})\text{Cl}]$  and the corresponding constant was close to the value of  $k_1$  obtained in the absence of  $\text{PPh}_3$ , showing only a small positive trend with the concentration of the phosphine (at  $[\text{PPh}_3] = 4 \times 10^{-3} \text{ mol dm}^{-3}$  the observed rate constant was  $0.40 \text{ min}^{-1}$ ).

*Type B experiments.* When  $\text{PPh}_3$  was added to the reaction solution after completion of the first step the absorbance at 653 nm showed an initial fast increase followed by a slower further increase. This behaviour is shown in Fig. 8 (inset).

Within the  $\text{PPh}_3$  concentration range  $2 \times 10^{-5}$ – $1.9 \times 10^{-4} \text{ mol dm}^{-3}$  and in the presence of a nearly constant water concentration ( $0.25 \text{ mol dm}^{-3}$ ), the final portion of the absorbance vs. time curve obeyed a first-order law (Fig. 8, empty circles) with a rate constant  $k_f = 0.22 \pm 0.06 \text{ min}^{-1}$ , independent of phosphine concentration.

Under the assumption of two consecutive, first-order processes, extrapolation to zero time of the absorbance curve (dotted line in Fig. 8) allowed the rate constant,  $k_i$ , of the first, fast process to be evaluated (filled circles). This rate constant appears to be a linear function of phosphine concentration ( $k_i = 1.0 \times 10^5 [\text{PPh}_3] \text{ min}^{-1}$ ).

Of the total increase in absorbance at 653 nm due to the fast and the slow reactions, about 30% ( $27 \pm 6\%$ ) was due to the first process.

*Formation of  $\text{OPPh}_3$ .* The above experiments, carried out under homogeneous conditions at very low iron complex concentrations, were not suitable for a search for the expected triphenylphosphine oxide. The formation of  $\text{OPPh}_3$  was instead demonstrated in the following way: 1.2 g of  $[\text{Fe}(\text{pc})\text{Cl}]$  (2.0 mmol) were suspended in py (10  $\text{cm}^3$ ) containing water (0.30  $\text{cm}^3$ ) and  $\text{PPh}_3$  (290 mg, 1.1 mmol) and the heterogeneous mixture stirred for *ca.* 3 h at room temperature. The solvent was then distilled off and the solid residue thoroughly dried. This material was extracted with anhydrous methanol, the solution filtered and the solvent eliminated by vacuum distillation. The

\* Rates  $R$  were obviously calculated as  $\Delta D_t/\Delta t$  ratios over finite time intervals. The corresponding  $x_A$  values were calculated using for  $D_i$  the middle point of the interval  $\Delta D_t$ .

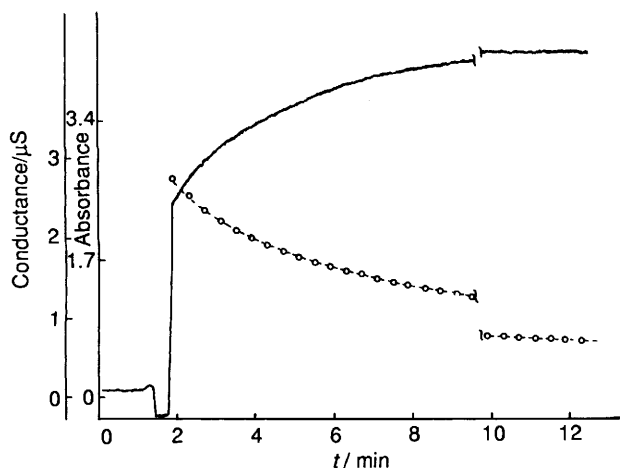


Fig. 9 Increase in conductance (continuous trace) and decrease in absorbance ( $\lambda = 688$  nm, circles) for a reacting solution immediately after mixing. No water added

IR spectrum of the solid residue showed the bands characteristic of an authentic sample of  $\text{OPPh}_3$ , whilst the absence of the strong bands at  $685$  and  $732\text{ cm}^{-1}$  of  $\text{PPh}_3$  was diagnostic of a nearly quantitative oxidation of the phosphine. A blank experiment showed that in the absence of  $[\text{Fe}(\text{pc})\text{Cl}]$  no IR-detectable  $\text{PPh}_3$  oxidation takes place, under comparable conditions. Microscope observation showed the presence of well shaped colourless crystals melting at  $152^\circ\text{C}$  (m.p. of  $\text{OPPh}_3$ :  $156^\circ\text{C}$ ).

**Conductometric Experiments.**—The results of a typical conductometric experiment are shown in Fig. 9. The addition of  $[\text{Fe}(\text{pc})\text{Cl}]$  to pure py results in an increase in conductance, indicating the formation of ions, and if the concomitant spectral changes are simultaneously recorded it is clear that the increase in conductance refers to the first step of the reaction. No changes in conductance are associated with the second step.

The procedure followed in these experiments (making and handling the solutions) required a dead time slightly longer than for the spectrophotometric experiments (*ca.* 15 s). This makes somewhat imprecise the direct measurement of the zero-time conductance. Nevertheless, inspection of Fig. 9 excludes that the conductance *vs.* time curve may extrapolate to the background conductance for  $t = 0$ . Hence, ions must be present at the start or they are formed *via* a fast reaction ( $t_{\frac{1}{2}} \leq 3$  s). A quantitative analysis of the conductance *vs.* time profile does indicate that a fast process is taking place upon mixing, which is responsible for the 'immediate' increase in conductivity.

## Discussion

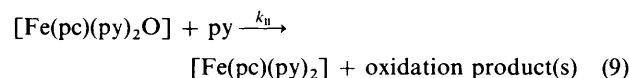
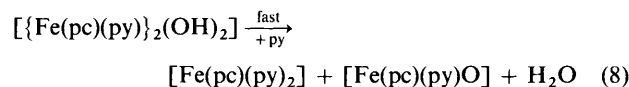
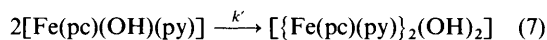
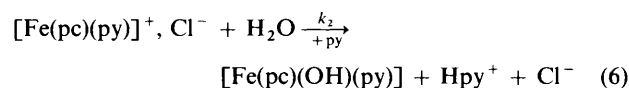
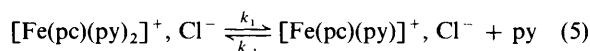
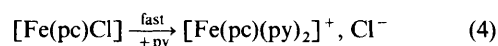
Phthalocyaninatoiron(III) complexes containing anions as axial ligands are not very common. In addition to  $[\text{Fe}(\text{pc})\text{Cl}]$ , the preparation and properties of  $[\text{Fe}(\text{pc})\text{X}]$  ( $\text{X} = \text{F}, \text{Br}$  or  $\text{I}$ ) have been reported.<sup>9</sup> Dicyano(phthalocyaninato)iron(III),<sup>16,17</sup> dihydroxo-, phenoxo-, cyanato- and -azido-(phthalocyaninato)iron(III)<sup>17</sup> and bis(alkoxo)(phthalocyaninato)iron(III)<sup>9</sup> salts of bulky cations have also been prepared. The existence of pairs of  $\text{I}_2$ -linked  $\text{Fe}^{\text{III}}(\text{pc})\text{Cl}$  units has been reported by Palmer *et al.*<sup>10</sup> No systematic study of the reactivity of these complexes has been carried out and only the reaction of  $[\text{Fe}(\text{pc})(\text{OR})]^-$  ( $\text{R} = \text{H}$  or alkyl) anions with water to give the well characterised  $\mu$ -oxo-bis(phthalocyaninato)iron(III) is cited.<sup>9</sup>

On the contrary, the reactivity of the related  $[\text{Fe}(\text{tpp})\text{X}]$  complexes (tpp = 5,10,15,20-tetraphenylporphyrinate;  $\text{X} = \text{F}, \text{Cl}$  or  $\text{N}_3$ ) has been thoroughly studied in the presence of coordinating bases such as imidazoles.<sup>18–21</sup> The release of  $\text{X}^-$  is strongly influenced by the presence of protic molecules (such as

imidazole itself) which act as catalysts through hydrogen bonding with the leaving anion.

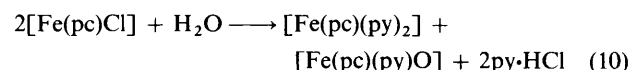
Thus, it is tempting to explain the linear dependence on water concentration shown by the pseudo-first-order rate constant for the first step in the present reaction with the same mechanism. According to this hypothesis,  $[\text{Fe}(\text{pc})\text{Cl}]$  should immediately give the six-co-ordinate species  $[\text{Fe}(\text{pc})\text{Cl}(\text{py})]$  which then should undergo a slow water-catalysed  $\text{Cl}^-$  substitution to give the cation  $[\text{Fe}(\text{pc})(\text{py})_2]^+$ . The latter would eventually be reduced by the pyridine,<sup>6</sup> thus accounting for the second step. However, the mechanism is likely to be more complex than this and the role of water different from that outlined above. It has been shown (see Results) that any reasonable extrapolation to zero time of the conductivity profile of Fig. 9 gives an initial value definitely higher than that of the pure solvent. Furthermore, it is known that the electronic spectrum of  $[\text{Fe}(\text{pc})]$  in the presence of various bases, such as pyridine, imidazole and some anions, shows a low-intensity band within the range  $400$ – $440$  nm.<sup>13,22</sup> This band, is characteristic of low-spin phthalocyaninatoiron(II) complexes having two strong-field axial ligands and is absent when only one axial ligand is strong-field. Thus, the band at  $414$  nm can be assumed to monitor the accumulation of the stable  $[\text{Fe}(\text{pc})(\text{py})_2]$  and, under such a hypothesis, Figs. 3 and 4 suggest that comparable amounts of this compound are produced during the first and the second step. This is also in agreement with the growth of the band at  $653$  nm which begins with the first step and goes to completion at the end of the second (Fig. 2).

These observations, as well as the 82% overall yield of  $[\text{Fe}(\text{pc})(\text{py})_2]$ , while hardly in agreement with the porphyrinato-like water-catalysed mechanism<sup>18–21</sup> are consistent with equations (4)–(8) (first step) and (9) (second step). Indeed, if



both intermediates  $[\text{Fe}(\text{pc})(\text{py})]^+, \text{Cl}^-$  and  $[\text{Fe}(\text{pc})(\text{py})(\text{OH})]$  are in a steady-state condition, reactions (4)–(8) describe, for the first step, an overall process which is first order in the concentrations of both  $[\text{Fe}(\text{pc})(\text{py})]^+, \text{Cl}^-$  and water (as observed), provided that  $k_2[\text{H}_2\text{O}] \ll k_{-1}[\text{py}]$ , the pseudo-first-order rate constant being  $k_1 = (k_1 k_2 / k_{-1})[\text{H}_2\text{O}]$ .

As shown in Fig. 6, the experimental kinetic law for the first step contains a term independent of water concentration that would not be predicted by the proposed scheme. However, this term is likely a consequence of the unavoidable presence of traces of water in the pyridine used. The overall reaction corresponding to the first step, as obtained by summing equations (4)–(8) would then be (10).



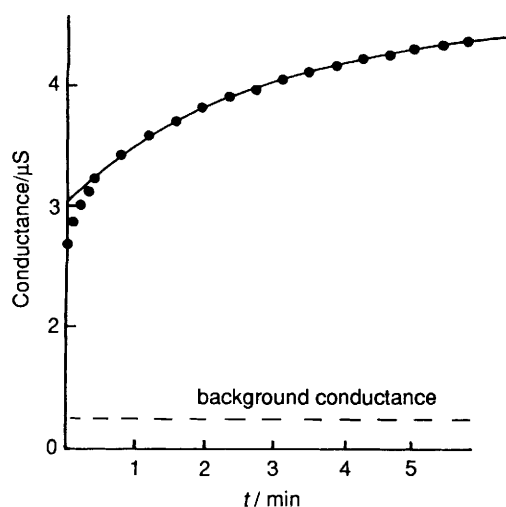


Fig. 10 Conductance vs. time profile of the first step at 35 °C. The continuous curve is calculated as described in the text. Circles are experimental values

The band at 688 nm is thus ascribed to the ion pair  $[\text{Fe}(\text{pc})(\text{py})_2]^+$ ,  $\text{Cl}^-$  and the presence of ions soon after mixing to its partial dissociation. Furthermore, whilst the optical changes observed for the first step would be due to the disappearance of  $[\text{Fe}(\text{pc})(\text{py})_2]^+$ ,  $\text{Cl}^-$ , to be replaced by  $[\text{Fe}(\text{pc})(\text{py})_2]$  and  $[\text{Fe}(\text{pc})(\text{py})\text{O}]$ , the change in conductance would be a consequence of the disappearance of  $[\text{Fe}(\text{pc})(\text{py})_2]^+$ ,  $\text{Cl}^-$  stoichiometrically replaced by pyridinium chloride. This last conclusion has been checked as follows. If a conducting species ACl reacts via a first-order process to give the conducting species BCl (A and B being in this case  $[\text{Fe}(\text{pc})(\text{py})_2]^+$  and  $\text{Hpy}^+$ , respectively), the conductance vs. time profile is described by equations (11) and (12) where  $c_0$  is the

$$\Gamma = c_0[\alpha_A(1-x)\Gamma_{0,A} + \alpha_B x \Gamma_{0,B}]10^{-3}/C + \Gamma_s \quad (11)$$

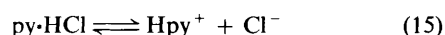
$$x = \exp(-k_1 t) \quad (12)$$

initial concentration of iron(III),  $\alpha_A$  and  $\alpha_B$  are the degrees of dissociation at any time  $t$  of the ion pair  $[\text{Fe}(\text{pc})(\text{py})_2]^+$ ,  $\text{Cl}^-$  and  $\text{py}\cdot\text{HCl}$ ,  $\Gamma_{0,A}$  and  $\Gamma_{0,B}$  their limiting molar conductivities, respectively,  $\Gamma_s$  the background conductance of the solvent and  $C$  the cell constant. Straightforward elaboration of the pertinent equilibrium equations gives, for  $\alpha_A$  and  $\alpha_B$ , (13) and (14). Two

$$\alpha_A = (K_A/K_B)\alpha_B/[1 - \alpha_B(1 - K_A/K_B)] \quad (13)$$

$$\alpha_B^3 c_0 (K_A/K_B - 1)(x - 1) + \alpha_B^2 \{K_A - K_B + c_0[x(K_A/K_B - 1) + 1]\} + \alpha_B(2K_B - K_A) - K_B = 0 \quad (14)$$

rather different values are reported for the equilibrium constant  $K_B$  of reaction (15),<sup>23</sup> i.e.  $8.7 \times 10^{-6}$  and  $7.1 \times 10^{-7}$  mol dm<sup>-3</sup>,



the latter obtained conductometrically. The value of  $K_B$  has been checked by measuring the conductance of pyridine solutions of known  $\text{py}\cdot\text{HCl}$  concentrations up to about  $1 \times 10^{-4}$  mol dm<sup>-3</sup>, giving  $(1.2 \pm 0.1) \times 10^{-6}$  mol dm<sup>-3</sup>, at 35 °C, in reasonable agreement with the previous value obtained with a similar procedure.

The limiting molar conductance of  $\text{py}\cdot\text{HCl}$  in pure pyridine is known<sup>23</sup> ( $\Gamma_{0,B} = 101.0$  S cm<sup>2</sup> mol<sup>-1</sup> at 25 °C). The limiting equivalent conductance of bulky cations under the same conditions ranges between 20 and 40 S cm<sup>2</sup> mol<sup>-1</sup>,<sup>23</sup> so that 30 S cm<sup>2</sup> mol<sup>-1</sup> may be considered as a reasonable estimate for the limiting molar conductance of the cation  $[\text{Fe}(\text{pc})(\text{py})_2]^+$ . This

sets the value of  $\Gamma_{0,A}$  to about 80 S cm<sup>2</sup> mol<sup>-1</sup> ( $\Gamma_{0,\text{Cl}} = 51.4$  S cm<sup>2</sup> mol<sup>-1</sup> at 25 °C, ref. 23).

A best-fit procedure based on equations (11)–(14) was followed, using the above values for  $K_B$ ,  $\Gamma_{0,A}$  and  $\Gamma_{0,B}$  and leaving  $k_1$  and  $K_A$  as adjustable parameters. Fig. 10 shows the experimental conductance of an  $[\text{Fe}(\text{pc})\text{Cl}]$  solution in pyridine with no added water as a function of time. The continuous curve is calculated assuming  $K_A = 5 \times 10^{-7}$  mol dm<sup>-3</sup> and  $k_1 = 0.26$  min<sup>-1</sup>. With the exception of the first few points, the fit is excellent and the value of the first-order rate constant is in good agreement with the average value measured spectrophotometrically (0.20 min<sup>-1</sup>, see Results). It is worth mentioning that this procedure, when applied to eight independent experiments, showed best-fit conditions for nearly identical values of  $K_A$  and  $k_1$ . It is also relevant that the final (end of the second step) concentration of  $[\text{Fe}(\text{pc})(\text{py})_2]$ , as measured by the absorption at 653 nm, was  $71 \pm 4\%$  of the concentration of  $\text{py}\cdot\text{HCl}$  as obtained from the equilibrium conductance of the solutions. Although this value is somewhat lower than the yield of  $[\text{Fe}(\text{pc})(\text{py})_2]$  measured spectrophotometrically, it confirms the quantitative transfer of the positive charge of  $[\text{Fe}(\text{pc})(\text{py})_2]^+$  to a hydrogen atom, as predicted by equation (10). Reaction (4) is assumed to be fast, but inspection of Fig. 10 shows that the calculated conductance extrapolates to a zero-time value definitely higher than the experimental one. This behaviour is systematic and indicates that reaction (4) is not 'instantaneous'. Assuming a first-order law, the half-life may be estimated to be of the order of 3–4 s, the process being virtually complete within 20–30 s. This rate may be compared with the uncatalysed rate of  $\text{Cl}^-$  release from  $[\text{Fe}(\text{tpp})\text{Cl}(\text{mim})]$  ( $\text{mim} = N$ -methylimidazole). The rate constant for this reaction has been reported to vary, at 25 °C, from 360 to 0.7 s<sup>-1</sup> according to the solvent,<sup>18</sup> the corresponding half-life ranging from 3 ms to 1 s. Unfortunately, these values refer to solvents structurally rather different from pyridine and also the ligand *trans* to Cl is different. However, they appear not to be in contrast with the estimated value for  $[\text{Fe}(\text{pc})\text{Cl}(\text{py})]$  in py.

Reaction (7) corresponds to the formation of a transient dihydroxide-bridged phthalocyaninato-iron(III) dimer. There are no reports in the literature of the existence of such a species; however, kinetic evidence for a porphyrin-iron(III) intermediate having this dihydroxide-bridged structure has been reported.<sup>24</sup>

The disproportionation character of reaction (8) is required by two facts: (a) the reduction of iron(III) to -(II) during the first step, which implies a simultaneous oxidation reaction, and (b) the occurrence of the second step where additional  $[\text{Fe}(\text{pc})(\text{py})_2]$  is formed. Any oxidation reaction involving species other than  $[\text{Fe}(\text{pc})(\text{py})_2]^+$  itself would hardly account for a successive reaction and, in any case, this latter would not affect the visible spectrum of the solutions.

A formally oxoiron(IV) compound is postulated as a product of reaction (8). Indeed, oxidation of  $[\text{Fe}(\text{pc})(\text{py})_2]^+$  might not necessarily involve the metal since phthalocyaninato complexes are known where the macrocycle is in the oxidised form of a radical monoanion.<sup>16,25–28</sup> However, this latter hypothesis does not seem to apply in the present case since a sample of  $[\text{Fe}(\text{pc})\text{Cl}_2]$ , which contains the  $\text{pc}^{\cdot-}$  radical,\* if dissolved in pyridine, gives immediately the visible spectrum and the reactivity behaviour of  $[\text{Fe}(\text{pc})\text{Cl}]$ .

Phthalocyaninatooxo complexes of metals such as  $\text{Mo}^{\text{IV}}$ ,<sup>29</sup>  $\text{Mn}^{\text{IV}}$ ,<sup>30</sup>  $\text{V}^{\text{IV}}$ <sup>31</sup> and  $\text{Cr}^{\text{IV}}$ <sup>32</sup> are also known or their existence has been claimed as reaction intermediates. However, there are no reports in the literature about phthalocyaninato-oxoiron(IV).

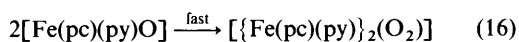
Porphyrinatooxoiron(IV) complexes are well known. They have been assumed to play an important role in the mechanism

\* This compound has been prepared according to the procedure described in ref. 25 and shows the same properties (elemental analysis, IR spectrum) as those reported.

of action of haem-type enzymes<sup>33</sup> and, recently, several compounds of this class have been generated by a variety of methods and characterised.<sup>33-44</sup> They are generally powerful oxidants and can only be handled in solution and at very low temperatures. They are also formed as photodisproportionation products of  $\mu$ -oxobis[(porphyrinato)iron(III)] complexes.<sup>40,45,46</sup>

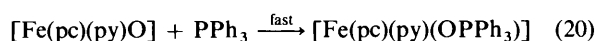
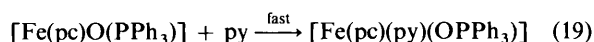
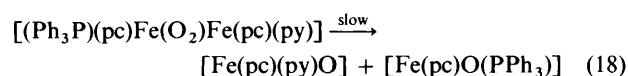
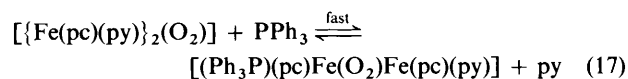
Thus, the accumulation of a relatively inert, ferryl-type compound under the reaction conditions of this work raises some questions. Preliminary attempts to detect in the IR spectrum of the reaction products the Fe=O stretching vibration band (expected<sup>32</sup> at about 1200  $\text{cm}^{-1}$ ) did not give conclusive results. Unfortunately, the low solubility of the [Fe(pc)Cl] and the lability of the iron(IV) intermediate place some limitations upon this approach. However, more accurate IR experiments, including the use of [<sup>18</sup>O]water, are projected in order to clarify this important point. It should also be mentioned that no IR evidence was found for the presence of pyridine *N*-oxide.<sup>47</sup>

An hypothesis which might reconcile the formation of an oxoiron(IV) compound with the need for a reasonable degree of inertness of the oxidised species accumulating during the first step is that the oxoiron(IV) dimerises rapidly giving either  $\mu$ -peroxy-bis[(phthalocyaninato)iron(III)] or a di- $\mu$ -oxo-bis[(phthalocyaninato)iron(IV)] [equation (16)], where the



oxygens should be less readily available for transfer to a reducing substrate.

The hypothesis of a dimer as the final oxidation product of the first step would also better explain a [Fe(pc)(py)<sub>2</sub>] yield lower than 100% and close to 75%. The bleaching of phthalocyaninatoiron solutions is obviously due to the destruction of the macrocycle and this requires the removal of at least two electrons from the ring.<sup>25</sup> The formation of [Fe(pc)(py)<sub>2</sub>] from the binuclear complex [Fe(pc)(py)<sub>2</sub>(O<sub>2</sub>)] would leave on the remaining part of the molecule an electron deficiency large enough to produce a deep decomposition of the ring. According to this reasoning, the overall yield of [Fe(pc)(py)<sub>2</sub>] should be 75%, in substantial agreement with the observations. The formation of triphenylphosphine oxide when the reaction is carried out in the presence of PPh<sub>3</sub> is strong evidence in favour of the formation of a ferryl-type intermediate. It is well known that the phosphine acts as an efficient oxygen-trapping agent towards the structurally similar oxoporphyrinatoiron(IV), giving OPPh<sub>3</sub> and the corresponding porphyrinatoiron(II).<sup>37,40,45,46,48</sup> Also the kinetic effects of added PPh<sub>3</sub> may be reconciled with the suggested mechanism. Thus, the type B experiments might be explained on the basis of equations (17)–(20) for the first phosphine-dependent process and equation (21) for the second, phosphine-independent reaction.



Type A experiments are also consistent with this interpretation. Under conditions where the reaction of [Fe(pc)Cl] with H<sub>2</sub>O–py–PPh<sub>3</sub> seems to take place in only one

step (*i.e.* for [PPh<sub>3</sub>]  $\geq 4 \times 10^{-3}$  mol dm<sup>-3</sup>) the phosphine-dependent process [equations (17)–(20)] is practically instantaneous ( $t_{\frac{1}{2}} \leq 0.8$  s). This means that, in the presence of relatively large amounts of PPh<sub>3</sub>, the oxidised product obtained during the first step would be [Fe(pc)(py)(OPPh<sub>3</sub>)]. Hence, the second step would correspond to reaction (21), in turn to be identified with the phosphine-independent reaction of type B experiments, and, since the latter has a rate constant very close to that of the first step, the whole process could well appear as occurring as a single kinetic step.<sup>14</sup> This interpretation is also consistent with the observed shift towards 100% yield of [Fe(pc)(py)<sub>2</sub>] when the reaction is carried out in the presence of PPh<sub>3</sub>.

There are two final points which are not fully understood at present, *i.e.* the effect of water on the spectrum at the end of the first step and the presence of the zero-order term in equation (2). Fig. 5 shows that on increasing [H<sub>2</sub>O] the strong charge-transfer band centred at 653 nm becomes progressively asymmetric. This effect does not seem to be related to any equilibrium involving the reaction products and water since the addition of the latter soon after the completion of the first step does not affect the spectrum in the way expected. Equally unclear is the origin of the zero-order term *b* in equation (2). Possibly, a slow reaction of an excess compound (pyridine itself or any impurity present therein at mmol dm<sup>-3</sup> concentration levels) yielding a product which reacts rapidly with [Fe(pc)(py)<sub>2</sub>(O<sub>2</sub>)] would lead to a kinetic term independent of the concentration of the latter.

Additional efforts are planned better to characterise the labile species produced during the reaction described. NMR and electrochemical experiments are being considered in order to gain additional information on this complex system.

### Acknowledgements

The significant contribution of Professor C. Ercolani to the discussion of the data is warmly acknowledged. Thanks are also due to Dr. M. Bassetti for his help in some preliminary IR experiments.

### References

- 1 P. A. Barrett, D. A. Frye and R. P. Lindstead, *J. Chem. Soc.*, 1938, 1157.
- 2 D. J. Ingram and J. E. Bennett, *Discuss. Faraday Soc.*, 1955, **19**, 140.
- 3 J. A. Elvidge, *J. Chem. Soc.*, 1961, 869.
- 4 A. B. P. Lever, *J. Chem. Soc.*, 1965, 1821.
- 5 M. Mossoyan-Deneux and D. Benlian, *Inorg. Nucl. Chem.*, 1981, **43**, 635.
- 6 A. B. P. Lever and J. P. Wilshire, *Inorg. Chem.*, 1978, **17**, 1145.
- 7 J. Sidorov and A. Terenin, *Opt. Spectros. (USSR)*, 1961, **11**, 175.
- 8 J. G. Jones and M. V. Twigg, *J. Chem. Soc. A*, 1970, 1546.
- 9 W. Kalz and H. Homborg, *Z. Naturforsch., Teil B*, 1983, **38**, 470.
- 10 S. M. Palmer, J. L. Stanton, N. K. Jaggi, B. M. Hoffman, J. A. Ibers and L. H. Schwartz, *Inorg. Chem.*, 1985, **24**, 2040.
- 11 B. J. Kennedy, G. Brain and K. S. Murray, *Inorg. Chim. Acta*, 1984, **81**, L29.
- 12 F. Monacelli, C. Ercolani and S. David, unpublished work.
- 13 B. W. Dale, *Trans. Faraday Soc.*, 1969, **65**, 331.
- 14 C. F. Bernasconi, *Relaxation Kinetics*, Academic Press, New York, 1976, ch. 9.
- 15 A. Frost and R. G. Pearson, *Kinetics and Mechanism*, 2nd edn., Wiley, New York, 1961, p. 49.
- 16 W. Kalz, H. Homborg, H. Kuppers, B. J. Kennedy and K. S. Murray, *Z. Naturforsch., Teil B*, 1984, **39**, 1478.
- 17 B. J. Kennedy, K. S. Murray, P. R. Zwack, H. Homborg and W. Kalz, *Inorg. Chem.*, 1986, **25**, 2539.
- 18 M. M. Doeff and D. A. Sweigart, *Inorg. Chem.*, 1984, **21**, 3699.
- 19 G. A. Tondreau and D. A. Sweigart, *Inorg. Chem.*, 1984, **23**, 1060.
- 20 J. G. Jones, G. A. Tondreau, J. O. Edwards and D. A. Sweigart, *Inorg. Chem.*, 1985, **24**, 296.
- 21 W. Byers, J. A. Cossham, J. O. Edwards, A. T. Gordon, J. G. Jones, E. T. P. Kenny, A. Mahmood, J. McKnight, D. A. Sweigart, G. A. Tondreau and T. Wright, *Inorg. Chem.*, 1986, **25**, 4767.

- 22 D. V. Stynes, *Inorg. Chem.*, 1977, **16**, 1170.
- 23 J.-M. Nigretto and M. Jozefowicz, *The Chemistry of Non-aqueous Solvents*, Academic Press, New York, 1978, vol. 5, p. 210.
- 24 J. R. Sutter, P. Hambright, P. B. Chock and M. Krishnamurthy, *Inorg. Chem.*, 1974, **13**, 2764.
- 25 J. F. Myers, G. W. Rayner Canham and A. B. P. Lever, *Inorg. Chem.*, 1975, **14**, 461.
- 26 B. Moubaraki, M. Ley, D. Benlian and J.-P. Sorbier, *Acta Crystallogr., Sect. B*, 1990, **46**, 379.
- 27 D. Dolphin, B. R. James, A. J. Murray and J. R. Thornback, *Can. J. Chem.*, 1980, **58**, 1125.
- 28 T. Nyokong, Z. Gasyna and M. J. Stillman, *Inorg. Chem.*, 1987, **26**, 548.
- 29 H. A. O. Hill and M. M. Norgett, *J. Chem. Soc. A*, 1966, 1476.
- 30 A. B. P. Lever, J. P. Wilshire and S. K. Quan, *Inorg. Chem.*, 1981, **20**, 761.
- 31 A. B. P. Lever, *Adv. Inorg. Chem. Radiochem.*, 1965, **7**, 27.
- 32 K. H. Nill, F. Wasgestian and A. Pfeil, *Inorg. Chem.*, 1979, **18**, 564.
- 33 J. T. Groves, R. Quinn, T. J. McMurry, M. Nakamura, G. Lang and B. Boso, *J. Am. Chem. Soc.*, 1985, **107**, 354.
- 34 D.-H. Chin, A. L. Balch and G. N. La Mar, *J. Am. Chem. Soc.*, 1980, **102**, 1446.
- 35 J. T. Groves, R. C. Haushalter, M. Nakamura, T. E. Nemo and B. J. Evans, *J. Am. Chem. Soc.*, 1981, **103**, 2884.
- 36 G. N. La Mar, J. S. de Ropp, L. Latos-Grazynski, A. L. Balch, R. B. Johnson, K. M. Smith, D. W. Parish and R.-J. Cheng, *J. Am. Chem. Soc.*, 1983, **105**, 782.
- 37 A. L. Balch, Y.-W. Chan, R.-J. Cheng, G. N. La Mar, L. Latos-Grazynski and M. W. Renner, *J. Am. Chem. Soc.*, 1984, **106**, 7779.
- 38 T. S. Calderwood, W. A. Lee and T. C. Bruice, *J. Am. Chem. Soc.*, 1985, **107**, 8272.
- 39 A. L. Balch, L. Latos-Grazynski and M. W. Renner, *J. Am. Chem. Soc.*, 1985, **107**, 2983.
- 40 M. W. Peterson and R. M. Richman, *Inorg. Chem.*, 1985, **24**, 722.
- 41 R. M. Richman and M. W. Peterson, *J. Am. Chem. Soc.*, 1982, **104**, 5795.
- 42 M. Schappacher, R. Weiss, R. Montiel-Montoya, A. Trautwein and A. Tabard, *J. Am. Chem. Soc.*, 1985, **107**, 3736.
- 43 K. Shin and H. M. Goff, *J. Am. Chem. Soc.*, 1987, **109**, 3140.
- 44 D. R. English, D. N. Hendrickson and K. S. Suslick, *Inorg. Chem.*, 1983, **22**, 367.
- 45 C. R. Guest, K. D. Straub, J. A. Hutchinson and P. M. Rentzepis, *J. Am. Chem. Soc.*, 1988, **110**, 5276.
- 46 M. W. Peterson, D. S. Rives and R. M. Richman, *J. Am. Chem. Soc.*, 1985, **107**, 2907.
- 47 G. Sartori, G. Costa and P. Blasina, *Gazz. Chim. Ital.*, 1955, **85**, 1085.
- 48 M. W. Peterson, D. S. Rivers and R. M. Richman, *J. Am. Chem. Soc.*, 1985, **107**, 2907.

Received 15th March 1991; Paper 1/01235E